Stochastic Strategies for a Swarm Robotic Assembly System

Loïc Matthey, Spring Berman and Vijay Kumar

***Abstract*—**

I. INTRODUCTION

We present an approach to designing a reconfigurable manufacturing system in which a swarm of homogeneous robots assembles static parts into different types of products. The system must respond quickly to produce desired amounts of products, which can change at discrete points in time, from any initial set of parts. Since it is difficult, if not impossible, to efficiently control a large robot population through centralized algorithms, we employ a decentralized strategy in which robots operate autonomously and use local communication. The strategy can be readily implemented on resource-constrained robots, and it is scalable in the number of robots and parts and robust to changes in robot population.

The robots move randomly within a closed arena, encountering parts and other robots at probability rates that are determined by the physical parameters of the system and by sensor and environmental noise. We model this behavior using a realistic 3D physics simulation, which we refer to as a *micro-continuous model* since it encompasses the continuous dynamics of individual robots. The system can be approximated as well-mixed, and the robot-part and robot-robot interactions are analogous to chemical reactions between molecules. Hence, like a set of chemical reactions, our system can be represented by the Stochastic Master Equation [1]. We call this the *macro-discrete model* because it describes a continuous-time Markov process whose states are the discrete numbers of system components. When there are large numbers of parts, the system can be abstracted to an ordinary differential equation (ODE) model, which we call a *macro-continuous model* since its state variables are continuous amounts of the parts.

Our work is similar in objective to studies on programmable self-assembly for modular robots [2]–[5]. The system in this work is a set of triangular robots that move around randomly on an air table and assemble into components according to a plan that is constructed using *graph grammars*, which are rules that define interactions between robots. Graph grammars can be constructed automatically to produce a given predefined assembly [5]. The probabilities of a newly formed component to detach into different combinations of parts can be optimized to maximize the number of a desired assembly at equilibrium [3]. However, this optimization requires the enumeration of all system states reachable from the initial state. In addition, the assembly plan relies on kinetic rate constants that must be measured from simulations.

Our approach to assembly system design allows for improved scalability and flexibility. We consider a scenario in which a heterogeneous set of parts is assembled into two types of final products. To provide theoretical guarantees on performance, we employ the "top-down" design methodology presented in [6]–[8] for reallocating a swarm of robots among a set of sites/tasks in a desired distribution. We first construct a *complete macro-continuous model* of the system using the Chemical Reaction Network framework [9], [10], which has been studied extensively for theoretical insight into biochemical systems. We compute reaction rate constants in the model from physical properties of the robots and environment and check that the model accurately predicts the results of the micro-continuous model. Then we simplify this abstraction to a *reduced macro-continuous model* with the same rates and use the model to optimize these rates for fast convergence to a target distribution of products, using a methodology similar to [11], [12]. The optimization problem is independent of the number of parts and scales only with the number of rates. We map the rates onto probabilities of assembly and disassembly and run the modified system on both the macro-discrete and microscopic models. The desired ratio of final products is achieved, although some tuning of the [WHICH?] model is needed to reduce discrepancies with the physical system.

[WILL PUT 3-LEVEL FIGURE HERE (?)]

II. PROBLEM STATEMENT

A. Assembly task

There are four different types of components, numbered 1 through 4, which can be combined to form larger components according to the assembly plans in Fig. 1. Components bond together through bi-directional connections at sites along their perimeters. The last step in each plan is the production of a final assembly, $F1$ or $F2$. The assembly task is executed by a group of robots in an arena that is sufficiently large to ignore the dynamics of small-scale interactions. Initially, robots and many copies of components of type 1 through 4 are randomly scattered. throughout the arena. There are exactly as many of these components as are needed to create a specified number of final assemblies, and the number of

L. Matthey is with the DISAL Laboratory, Ecole Polytechnique Federale de Lausanne, Station 14, 1015 Lausanne, Switzerland, loic.matthey@epfl.ch

S. Berman and V. Kumar are with the GRASP Laboratory, University of Pennsylvania, 3330 Walnut Street, Philadelphia, PA 19104, USA, {spring, kumar}@grasp.upenn.edu

We gratefully acknowledge partial support from NSF grants CSR-CPS 0720801, IIS-0427313, NSF IIP-0742304, and IIS-0413138, ARO grant W911NF-05-1-0219, and ONR grant N00014-07-1-0829.

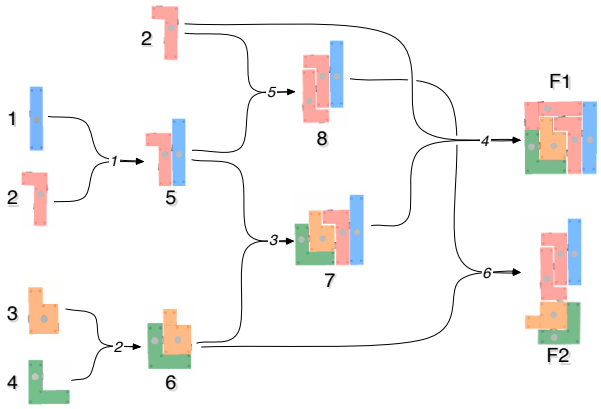

Fig. 1. Assembly plans for final assemblies F1 and F2.

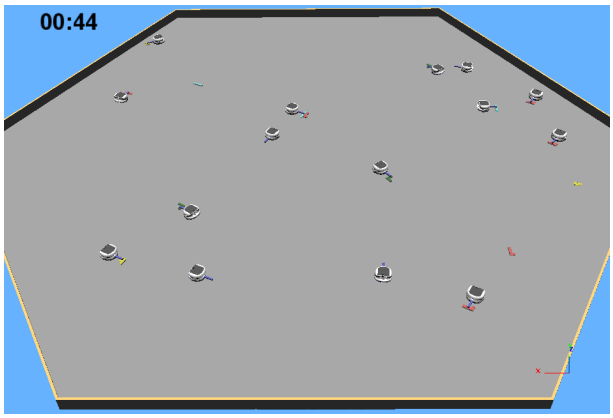

Fig. 2. Snapshot of the arena in the realistic physical simulation. Robots carry parts at the end of a protruding bar.

robots equals the total number of scattered components. Each robot knows the assembly plans a-priori and has the ability to recognize component types, pick up a component, combine it with one that is being carried by another robot, and disassemble a component it is carrying.

Our objective is to define robot controllers for moving around the arena and for picking up, assembling, and disassembling components so that the robots produce target numbers of final assemblies as quickly as possible.

B. Micro-continuous model

We implement the assembly task in the robot simulator Webots [13], which uses the Open Dynamics Engine to accurately simulate physics. We use the robot platform Khepera III, which has infra-red distance sensors for collision avoidance. Each robot is outfitted with a protruding bar with a rotational servo at the tip. A magnet on the servo bonds to a magnet on the top face of a part, and the servo is used to rotate the bonded part into the correct orientation for assembly. Parts bond to each other via magnets on their side faces. Magnets can turned off to deactivate a bond. Robots and parts are equipped with a radio emitter and receiver for local communication and for computing relative bearing, which is used to align robot and part magnets and to rotate a part for assembly. The task takes place inside the walled hexagonal arena shown in Fig. 2.

We use a control policy for the robots that is inspired by chemical processes: random movement patterns with probabilistic assemblies upon encounter, as well as random disassemblies. Our models assume that the system is well-mixed; to achieve this property, robots move according to a random walk, and we verify that the space is uniformly covered. Robots and parts switch between action states based on information they receive via local sensing and communication. When a robot encounters a part on the ground, it approaches and bonds to it and starts searching for a robot that is carrying a compatible part, according to the assembly plans. When one is found, the two robots align their parts and approach each other to join the parts. One robot carries off the newly assembled part while the other resumes searching for a part on the ground. A robot can disassemble a part it is carrying by dropping one of the component parts on the floor. To control the outcome of part populations, we can directly modify the probabilities of starting an assembly or performing a disassembly.

III. MACRO-CONTINUOUS MODELS

A. Definitions

Interactions between parts and robots in the assembly system are modeled in the form of a Chemical Reaction Network (CRN). A set of reactions can be represented as a directed graph, $\mathcal{G} = (\mathcal{V}, \mathcal{E})$. The set of vertices, $\mathcal{V}$, signifies the *complexes*, which are the combinations of parts and/or robots that appear before and after reaction arrows. The set of directed edges, $\mathcal{E}$, represents the reaction pathways between the complexes. Each pathway is denoted by an ordered pair $(i, j) \in \mathcal{V} \times \mathcal{V}$, which means that that complex i transforms into complex j, and is associated with a positive *reaction rate constant*.

Each part of type i in Fig. 1 is symbolized by X_i, and a robot is symbolized by X_R. X_i may be further classified as X_i^u, an unclaimed part on the ground, or as X_i^c, a claimed part i and the robot that is carrying it. Let M be the number of these variables, or *species*, in a model of the system. Then $\mathbf{x}(t) \in \mathbb{R}^M$ is the vector of the species populations, which are represented as continuous functions of time t.

B. Complete macro-continuous model

We define a CRN that represents each possible action in the micro-continuous model of the assembly system:

$$
\begin{array}{cc}
X_R + X_1^u \xrightarrow{e_1} X_1^c & X_R + X_5^u \xrightarrow{e_5} X_5^c \\
X_R + X_2^u \xrightarrow{e_2} X_2^c & X_R + X_6^u \xrightarrow{e_6} X_6^c \\
X_R + X_3^u \xrightarrow{e_3} X_3^c & X_R + X_7^u \xrightarrow{e_7} X_7^c \\
X_R + X_4^u \xrightarrow{e_4} X_4^c & X_R + X_8^u \xrightarrow{e_8} X_8^c \\
X_1^c + X_2^c \xrightarrow{k_1^+} X_5^c + X_R & X_2^c + X_7^c \xrightarrow{k_4^+} X_{F1}^c + X_R \\
X_3^c + X_4^c \xrightarrow{k_2^+} X_6^c + X_R & X_2^c + X_5^c \xrightarrow{k_5^+} X_8^c + X_R \\
X_5^c + X_6^c \xrightarrow{k_3^+} X_7^c + X_R & X_6^c + X_8^c \xrightarrow{k_6^+} X_{F2}^c + X_R \\
X_5^c \xrightarrow{k_1^-} X_1^c + X_2^u & X_{F1}^c \xrightarrow{k_4^-} X_7^c + X_2^u \\
X_6^c \xrightarrow{k_2^-} X_3^c + X_4^u & X_8^c \xrightarrow{k_5^-} X_5^c + X_2^u \\
X_7^c \xrightarrow{k_3^-} X_6^c + X_5^u & X_{F2}^c \xrightarrow{k_6^-} X_8^c + X_6^u
\end{array}
\qquad (1)
$$

In this CRN, e_i is the rate at which a robot encounters a part of type i, k_i^+ is the rate of assembly process j, and k_i^- is the rate of disassembly process j. We theoretically estimate these rates as functions of the following probabilities:

$$e_i = p^e \ , \qquad k_i^+ = p^e \cdot p_i^a \cdot p_i^+ \ , \qquad k_i^- = p_i^- \ . \qquad (2)$$

p^e is the probability that a robot encounters a part or another robot. Using the assumption that robots and parts are distributed uniformly throughout the arena, we calculate p^e from the geometrical approach that is used to compute probabilities of molecular collisions [14]–[19]: $p^e \approx vTw/A$, where v is the average robot speed, T is a timestep, A is the area of the arena, and w is twice a robot's communication radius, since this is the range within which a robot detects a part or robot and initiates an assembly process.

p_i^a is the probability of two robots successfully completing assembly process i; it depends on the part geometries.

p_i^+ is the probability of two robots starting assembly process i, and p_i^- is the probability per unit time of a robot performing disassembly process i. These are the *tunable parameters* of the system.

We compute p_i^a and the parameters for p^e using measurements from the micro-continuous model (Webots simulations): $A = 23.38\ m^2$ (hexagon of radius 3m), $w = 1.2\ m$, $v_R = 0.128\ m/s$ from an average over 50 runs, and $\mathbf{p^a} = [0.9777\ 0.9074\ 0.9636\ 0.9737\ 0.8330\ 1.0]$ (entries follow the numbering of the associated reactions) from averages over 100 runs. We set $T = 1\ s$.

In the thermodynamic limit, which includes the condition that populations approach infinity, the physical system represented by (1) can be abstracted to an ODE model [20]. This is illustrated in the next section. We numerically integrate this macro-continuous model with the rates we calculated and also use the StochKit toolbox [21] to efficiently perform a stochastic simulation of the macro-discrete model. We compare the results to those for the micro-continuous model in Fig. 3, for $p_i^+ = 1$, $p_i^- = 0 \ \ \forall i$. The results for all

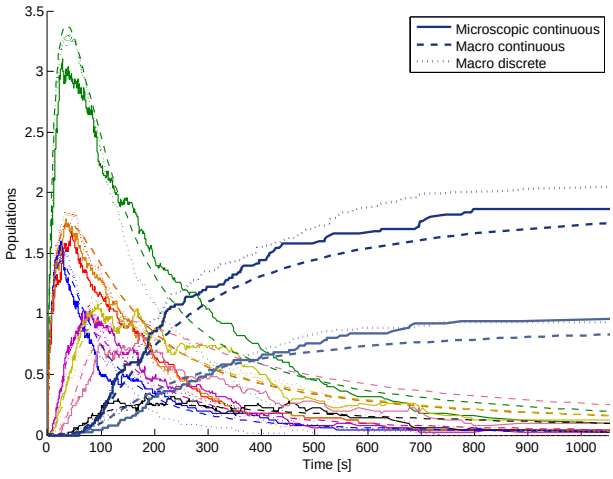

Fig. 3. Part populations in the complete macro-continuous, macro-discrete, and micro-continuous models for 3 final assemblies and 15 robots. Macro-discrete and micro-continuous results are averaged over 100 runs.

models are very similar, although discrepancies arise from two factors. First, certain events that happen in the physical simulation are not modeled: parts sticking together or being wedged against a wall, and deviations from the assumption of uniform spatial distribution. Second, the ODE approximation is valid only for large numbers of parts, and the system modeled had only 15 robots and 15 parts. Overall, the macro-continuous model accurately predicts the evolution of part populations, and hence we can use it to design the rates to direct the system's behavior, provided that the system has very large numbers of parts.

C. Reduced macro-continuous model

We simplify the complete model by abstracting away robots and retaining only interactions between parts, assuming that the time to find a part is small and we have more robots than parts:

$$
\begin{array}{cc}
X_1 + X_2 \underset{k_1^-}{\overset{k_1^+}{\rightleftharpoons}} X_5 & X_2 + X_7 \underset{k_4^-}{\overset{k_4^+}{\rightleftharpoons}} X_{F1} \\
X_3 + X_4 \underset{k_2^-}{\overset{k_2^+}{\rightleftharpoons}} X_6 & X_2 + X_5 \underset{k_5^-}{\overset{k_5^+}{\rightleftharpoons}} X_8 \\
X_5 + X_6 \underset{k_3^-}{\overset{k_3^+}{\rightleftharpoons}} X_7 & X_6 + X_8 \underset{k_6^-}{\overset{k_6^+}{\rightleftharpoons}} X_{F2}
\end{array}
\qquad (3)
$$

The rates are also defined by equation (2). This model converges to the same equilibria as the complete model [CHECK NEW], but its transient regime differs since we removed the delays that arise from robot interactions with free components and other robots.

We define a vector $\mathbf{y}(\mathbf{x}) \in \mathbb{R}^{12}$ in which entry y_i is the component or product of components in complex i:

$$
\begin{aligned}
\mathbf{y}(\mathbf{x}) = \quad & [x_1 x_2 \ \ x_5 \ \ x_3 x_4 \ \ x_6 \ \ x_2 x_7 \ \ x_{F1} \\
& x_5 x_6 \ \ x_7 \ \ x_2 x_5 \ \ x_8 \ \ x_6 x_8 \ \ x_{F2}]^T \ . \qquad (4)
\end{aligned}
$$

We also define a matrix $\mathbf{M} \in \mathbb{R}^{10\times 12}$ in which each entry M_{ji}, $j = 1, ..., 10$, of column $\mathbf{m}_i$ is the coefficient of

part type j in complex i (0 if absent). We relabel the rate associated with reaction $(i,j) \in \mathcal{E}$ as k_{ij} and define a matrix $\mathbf{K} \in \mathbb{R}^{12\times 12}$ with entries

$$K_{ij} = \begin{cases} k_{ji} & \text{if} \quad i \neq j \ , \quad (j,i) \in \mathcal{E} \ , \\ 0 & \text{if} \quad i \neq j \ , \quad (j,i) \notin \mathcal{E} \ , \\ -\sum_{(i,l)\in\mathcal{E}} k_{il} & \text{if} \quad i = j \ . \end{cases} \tag{5}$$

Then our ODE abstraction of the system can be written in the following form [22]:

$$\dot{\mathbf{x}} = \mathbf{MKy}(\mathbf{x}) \ . \tag{6}$$

One set of linearly independent conservation constraints on the part quantities is:

$$\begin{array}{lcl} x_3 - x_4 & = & N_1 \\ x_1 + x_5 + x_7 + x_8 + x_{F1} + x_{F2} & = & N_2 \\ x_2 + x_5 + x_7 + 2(x_8 + x_{F1} + x_{F2}) & = & N_3 \\ x_3 + x_6 + x_7 + x_{F1} + x_{F2} & = & N_4 \end{array} \tag{7}$$

where N_i, $i = 1, ..., 4$, are computed from the initial part quantities.

Theorem 1: System (6) subject to (7) has a unique, stable equilibrium $\bar{\mathbf{x}} > \mathbf{0}$.

Proof: Each equilibrium of the system, $\{\bar{\mathbf{x}} \mid \mathbf{MKy}(\bar{\mathbf{x}}) = \mathbf{0}\}$, can be classified as either a *positive* equilibrium $\bar{\mathbf{x}} > \mathbf{0}$ or a *boundary* equilibrium in which $\bar{x}_i = 0$ for some i, which can be found by solving $\mathbf{y}(\bar{\mathbf{x}}) = \mathbf{0}$ [22]. From definition (4) of $\mathbf{y}(\mathbf{x})$, it can be concluded that in each boundary equilibrium, all $x_i = 0$ except for one of the four combinations of variables $(x_1, x_3), (x_1, x_4), (x_2, x_3), (x_2, x_4)$. Since we only consider systems that can produce x_{F1} and x_{F2}, it is not possible for the system to reach any of these equilibria; each one lacks two component types needed for the final assemblies.

The *deficiency* δ of a reaction network is the number of complexes minus the number of linkage classes, each of which is a set of complexes connected by reactions, minus the network rank, which is the rank of the matrix with rows $\mathbf{m}_i - \mathbf{m}_j$, $(i,j) \in \mathcal{E}$ [23]. Network (3) has 12 complexes, 6 linkage classes, and rank 6; hence, $\delta = 0$. Also, the network is *weakly reversible* because whenever there is a directed arrow pathway from complex i to complex j, there is one from j to i. Because the network has deficiency 0, is weakly reversible, and does not admit any boundary equilibria, it has a unique, globally asymptotically stable positive equilibrium according to Theorem 4.1 of [24]. ■

IV. RATE OPTIMIZATION

We consider the problem of designing the system described by model (6) subject to (7) to produce desired quantities of components as quickly as possible. The objective will be posed as the design of *optimal rates* k_i^+, k_i^-, $i = 1, ..., 6$, which define an *optimal rate matrix* $\mathbf{K}^*$ according to (5), that minimize the convergence time of the system to a vector of target component quantities, $\mathbf{x^d}$. Note that although only the amounts of the final assemblies $F1$ and $F2$ may need to be specified in practice, our optimization problem requires that target quantities of *all* components be defined.

We first specify $x_1^d, x_2^d, x_3^d, x_5^d, x_8^d$ and a parameter

$$\alpha \equiv x_{F1}^d / (x_{F1}^d + x_{F2}^d) \ . \tag{8}$$

Then we compute the dependent variables x_4^d, x_6^d, x_7^d, and $x_{F1}^d + x_{F2}^d$ from the conservation equations (7) and definition (8) and check that they are positive to ensure a valid $\mathbf{x^d}$. In this way, we can keep $x_{F1}^d + x_{F2}^d$ and the target non-final component quantities constant while adjusting the ratio between x_{F1} and x_{F2} using α. Theorem 1 shows that we can achieve $\mathbf{x^d}$ from any initial distribution $\mathbf{x^0}$ by specifying that $\bar{\mathbf{x}} = \mathbf{x^d}$ through the following constraint on $\mathbf{K}$,

$$\mathbf{MKy}(\mathbf{x^d}) = \mathbf{0} \ . \tag{9}$$

Now we consider the aspect of minimizing the convergence time to $\mathbf{x^d}$. We quantify this time in terms of the system *relaxation times* τ_i, $i = 1, ..., 6$, the times in which different modes (dynamically independent variables) of the the system converge to a stable equilibrium after perturbation [25], [26]. Various measures of the average relaxation time of a CRN have been defined, but they are applicable only under certain conditions, such as a linear reaction sequence [27]. For instance, one such measure was minimized in the optimization of rates for the linear chain in [28].

To estimate the relaxation times, we first reformulate the system in terms of new variables. Define v_i, $i = 1, ..., 6$, as the difference between the forward and reverse fluxes associated with reaction i in system (3). For example, $v_1 = k_1 x_1 x_2 - k_2 x_5$. Let $\mathbf{v}(\mathbf{x}) = [v_1 \ ... \ v_6]^T$ and let $\mathbf{S} \in \mathbb{R}^{6\times 10}$ denote the stoichiometric matrix of the system, which is defined such that model (6) can be written as [29]:

$$\dot{\mathbf{x}} = \mathbf{Sv}(\mathbf{x}) \ . \tag{10}$$

The dynamical properties of a CRN are often analyzed by linearizing the ODE model of the system about an equilibrium and studying the properties of the associated Jacobian matrix $\mathbf{J} = \mathbf{SG}$, where the entries of $\mathbf{G}$ are $G_{ij} = dv_i/dx_j$ [26]. Denoting the eigenvalues of $\mathbf{J}$ by λ_i, a common measure of relaxation time is $\tau_i = 1/|Re(\lambda_i)|$. Since the λ_i are negative at a stable equilibrium, one way to yield fast convergence is to choose rates that minimize the largest λ_i. However, in our system it is very difficult to find analytical expressions for the λ_i. We use an alternative estimate of relaxation time that is also derived by linearizing the system around its equilibrium $\mathbf{x^d}$ [29],

$$\tau_j = \left(\sum_{i=1}^{10} (-s_{ij}) \frac{dv_j}{dx_i} \right)^{-1}_{\mathbf{x}=\mathbf{x^d}} \ . \tag{11}$$

Each reaction j in system (3) is of the form $X_k + X_l \rightleftharpoons^{k_j^+}_{k_j^-} X_m$. Thus, $v_j = k_j^+ x_k x_l - k_j^- x_m$, and the entries of column j in $\mathbf{S}$ are all 0 except for $s_{kj} = s_{lj} = -1$ and $s_{mj} = 1$. Then according to equation (11), the relaxation time for each reaction is

$$\tau_j = (k_j^+ (x_k^d + x_l^d) + k_j^-)^{-1} \ . \tag{12}$$

Define $\mathbf{k} \in \mathbb{R}^{12}$ as the vector of all rates k_i^+, k_i^-. Using equation (12), we define two possible objective functions $f : \mathbb{R}^{12} \to \mathbb{R}$, the average τ_j^{-1} and the minimum τ_j^{-1}, to *maximize* in order to produce fast convergence to $\mathbf{x^d}$:

$$f_{ave}(\mathbf{k}) = \frac{1}{6}\sum_{j=1}^{6} \tau_j^{-1} , \quad (13)$$

$$f_{min}(\mathbf{k}) = \min\{\tau_1^{-1}, \ldots, \tau_6^{-1}\} . \quad (14)$$

Finally, we write the rates k_i^+, k_i^- in terms of the tunable probabilities p_i^+, p_i^- using equation (2) and define these probabilities as the optimization variables. Let $\mathbf{p} \in \mathbb{R}^{12}$ be the vector of all p_i^+, p_i^-. Then the optimization problem can be posed as **Problem P** below. It will be referred to as **Problem P1** when $f = f_{ave}$ and as **Problem P2** when $f = f_{min}$.

$$\textbf{[P]} \quad \begin{aligned} &\text{maximize} && f(\mathbf{k}(\mathbf{p})) \\ &\text{subject to} && \mathbf{MK}(\mathbf{p})\mathbf{y}(\mathbf{x^d}) = \mathbf{0}, \quad \mathbf{0} \leq \mathbf{p} \leq \mathbf{1} . \end{aligned}$$

Problems P1 and P2 are both linear programs, which can be solved efficiently. To check that they do in fact minimize convergence time, we implemented a Monte Carlo method [30], which is more computationally expensive, to find the $\mathbf{k}(\mathbf{p})$ that directly minimizes this time. We measure the degree of convergence to $\mathbf{x^d}$ by $\Delta(\mathbf{x}) = ||\mathbf{y}(\mathbf{x}) - \mathbf{y}(\mathbf{x^d})||_2$ and say that one system converges faster than another if it takes less time for $\Delta(\mathbf{x})$ to decrease to some small fraction, here defined as 0.1, of its initial value. At each iteration, $\mathbf{k}(\mathbf{p})$ is perturbed by a random vector and projected onto the null space of linearly independent rows of a matrix $\mathbf{N}$ defined such that $\mathbf{Nk} = \mathbf{MK}\mathbf{y}(\mathbf{x^d}) = \mathbf{0}$. Once $\mathbf{k}(\mathbf{p})$ also satisfies $\mathbf{0} \leq \mathbf{p} \leq \mathbf{1}$, it is used to simulate the reduced macro-continuous ODE model to find $\Delta(\mathbf{x})$ after some time. Since the system is stable by Theorem 1, $\Delta(\mathbf{x})$ always decreases monotonically with time, so a Newton scheme can be used to compute the exact time when $\Delta(\mathbf{x}) = 0.1\Delta(\mathbf{x^0})$.

V. RESULTS

A. Optimization of rates

We apply our optimization method, for problems P1 and P2, for $\alpha \in \{0.01, \ldots, 0.99\}$. The obtained rates successfully create all desired α by varying only the rates of reactions 4 and 5 as a function of α, all others being constant, see Table V-A. This means that the system is flexible enough to create any ratio α by modifying only the two final reactions, which follows the Occam's razor principle.

To verify the effect of the optimization on the rate of convergence, we show the time evolution of the ratios for two different targets: $\alpha = 0.4$ and $\alpha = 0.8$, see Fig. 4. The rates found by solving Problem P1, Problem P2 and a non-optimal solution are used. The non-optimal solution satisfies the constraints on the equilibrium, but is not optimized with respect to the convergence time. Plot is shown with a logarithmic time-scale, for a ODE model simulation with 60 target assemblies.

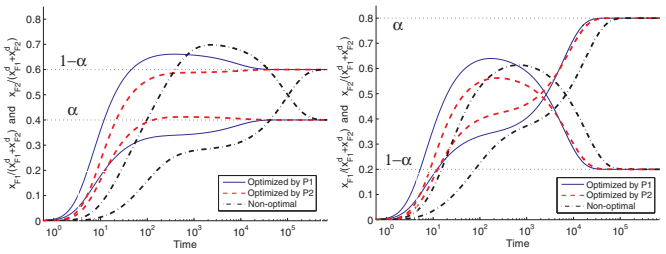

Fig. 4. Time evolution of ratio for desired ratios $\alpha = 0.4$ and $\alpha = 0.8$. Use optimized rates given by solving problem P1 and P2. Comparison with non-optimal set of rates.

We see that the target ratios are attained by all sets of rates. The two sets obtained by our optimization method converge faster to the solution. For $\alpha = 0.4$, the non-optimal set of rates undergoes a flipping of ratios at $t = 10^5$. This means that before that time, the system is far from the desired solution. On the other hand, the two optimized sets are converging to a better transient solution before attaining the desired equilibrium. This flipping discrepancy is not happening for $\alpha = 0.8$ as they all flip, but we still see a faster convergence of the optimized sets compared to the non-optimal one. Both objective functions used in Problems P1 and P2 seem good heuristics with respect to convergence time. Both have comparable performances, so we cannot decide between the two objectively.

B. Mapping on the micro-continuous model

We use the rates obtained by solving Problem P1 for $\alpha = 0.4$ for the micro-continuous model. As we found those rates using the reduced system, it is to be verified that the mapping of those rates gives rise to a valid solution. The robots are taking random biased decisions in order to ensure the optimized rates values. We show the average ratios attained for 30 simulated runs of 23 minutes, with random initial position and orientations for robots and pieces. We consider the rates of Problem P1 and of the non-optimal set. In Fig. 5, we see a similar trend to Fig. 4: convergence to the target ratios, with the non-optimal set showing a flipping of ratios. On the bad side, the convergence is not significantly different now, and the populations are varying more.

Problems due to bad modeling of some low-level effects could explain those results. In the micro-continuous model, when a piece is disassembled, it falls on the ground on the spot, which tends to improve the rate of re-assembly of the previous disassembled compound. This breaks the well-mixed assumption. The time to re-carrying of pieces by roaming robots is also affecting the results, as this was the abstracted part leading to the reduced system. Adding more free robots tends to minimize this effect.

C. Green manufacturing

We show an application of our findings to a reconfiguration task. We perform a simulation run where we change the goal under way. Namely, we change the target ratio of final assemblies F1 and F2.

TABLE I

VALUES OF OPTIMIZED RATES FOR VARYING α. *Continuous* RATES EVOLVE CONTINUOUSLY WITH RESPECT TO α.

Reaction i	**1**	**2**	**3**	**4**	**5**	**6**
P1 Optimized $\mathbf{p_i^+}$	1.0					
P1 Optimized $\mathbf{p_i^-}$	0.01885	0.00754	0.00377	*continuous*	0.00942	*continuous*
P2 Optimized $\mathbf{p_i^+}$	0.36	0.666	1.0	*continuous*	0.4705	*continuous*
P2 Optimized $\mathbf{p_i^-}$	0.006855	0.005027	0.00377	*continuous*	0.00443	*continuous*

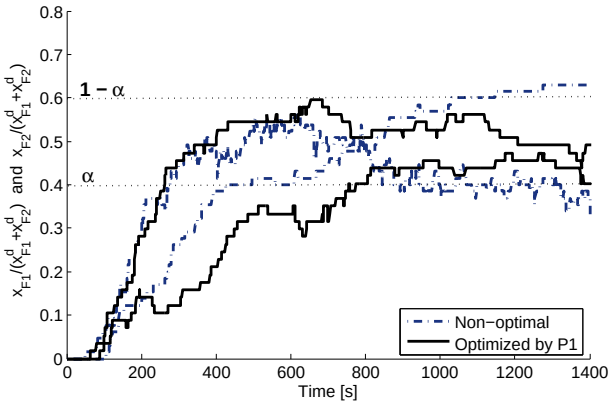

Fig. 5. Time evolution of ratios for $\alpha = 0.4$, in the micro-continuous model

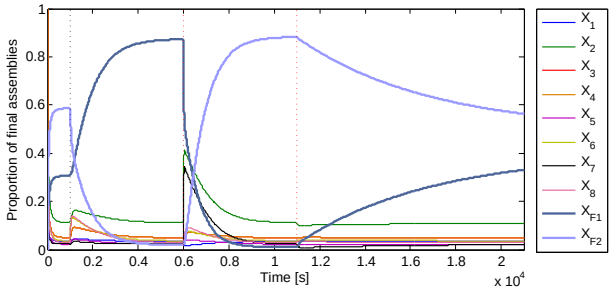

Fig. 6. Online adaptation to change of high-order goals by the assembly platform. Change in goals are shown at the dashed red lines.

This high-order goal is directly realizable by changing abruptly the set of reaction rates used by the robots. An example is shown in Figure 6, for rates optimized by Problem P1 and an ODE simulation with 60 target assemblies.

We see a quick adaptation to new high-order goals. Some goals are harder to attain (e.g. $\alpha = 0.5$), but high-level control is possible in real-time.

VI. DISCUSSION AND FUTURE WORK

We have shown an approach to designing a decentralized control policy to control a swarm of robots performing an assembly task. We first presented our models, which take advantage of a multi-level modeling methodology. A micro-continuous model implemented using a realistic physic simulator is abstracted two times to attain a level where our optimization is possible. Secondly, we shown our optimization methodology, which relies on global stability properties of a specific class of CRN, which our reduced model belongs to. We implement the optimization as a convex program, with constraints on the desired equilibrium values for every sub-assembly. We proposed two objective functions, using an heuristic approximation of the convergence time of the whole chemical reaction network to its equilibrium. Third we showed the results of such optimizations. Target α ratios are attained quicker than using a non-optimal set of rates. Yet we still need to compare those results with other optimization techniques, in order to assess the validity of our heuristic objective functions. Finally, we used the optimized set of rates and probabilities back onto the micro-continuous model. We found that, even while being optimized in an abstracted model, the rates create the desired goals. Discrepancies appeared, due in our opinion to violation of the well-mixed property and physic simulation problems.

Further works will need to compare the optimization scheme we propose to other ones, as well as assessing the relation between our objective functions and the convergence time of the overall system. A way to determine the desired equilibrium in a more flexible way is also needed. Right now we have to define every of its components, yet only a few of them are really of interest.

On another level, we do not address in this work the discrete optimal design of the assembly plans to create the target assemblies. The choice of an assembly plan creates the architecture of the chemical reaction network used in further steps. Further more, it controls the actions and steps available to create our target assemblies. Choosing it wisely is therefore of first importance, and we wish to study if we can directly apply our continuous optimization scheme for that purpose.

—

Such a methodology is only possible because we can make the complete macro model fit closely to the real data, and then go to the reduced macro model without losing much precision.

in the probabilistic sense - as N increases ...

, which define the individual robot controllers,

collective behavior of the system generally reflects the desired global properties,

In this way, we systematically derive individual robot controllers that guarantee desired aggregate properties of the system.

We do not address directly in this work the discrete optimal design of this Chemical Reaction Network.

The complete problem of constructing a final assembly from initial parts can be divided into two parts: a discrete and a continuous one.

1) The discrete part consists of the assembly plan itself. It

represents a finite and discrete set of rules to construct the final target.

2) The continuous part is the rate of evolution of the assembly, driven by the assembly plan but subject to continuous reaction rates. Those rates can take continuous values which will affect the final outcome of the assembly.

We wish then to study the optimization of these continuous reaction rates, as we think they might give more insight on the relations between parts of the plan and as they encompass the same power than the discrete part.

In order to go in that direction completely, one would need to consider the "full assembly plan". Such a plan would consists of every possible assembly steps towards the creation of a final assembly. Indeed, it would become quite big quickly, but pruning is possible, mainly because we assume that we have heterogenous pieces that have highly specific assembling sites. Such a plan is easily obtained using any enumeration method, for example Plya enumeration [31].

But in this work, we only consider a subset of this "full assembly plan". We assume that we are given a part of this plan, which already creates the final assembly. We then study only the effect of the reactions rates on this plan, and see what parts of it an optimization technique will push forward or cut down. This is an assumed simplification for the current work.

- Optimizing the plan using an expanded model

REFERENCES

[1] D. Gillespie, "A general method for numerically simulating the stochastic time evolution of coupled chemical reactions," *J. Comput. Phys.*, vol. 22, pp. 403–434, 1976.

[2] J. Bishop, S. Burden, E. Klavins, and R. Kreisberg, "Programmable parts: a demonstration of the grammatical approach to self-organization," *Intelligent Robots and Systems*, Jan 2005.

[3] E. Klavins, "Programmable self-assembly," *Control Systems Magazine*, Jan 2007.

[4] J. McNew, E. Klavins, and M. Egerstedt, "Solving coverage problems with embedded graph grammars," *Hybrid Systems: Computation and Control*.

[5] E. Klavins, R. Ghrist, and D. Lipsky, "A grammatical approach to self-organizing robotic systems," *Urbana*.

[6] S. Berman, A. Halasz, V. Kumar, and S. Pratt, "Algorithms for the analysis and synthesis of a bio-inspired swarm robotic system," *Swarm Robotics SAB 2006 International Workshop*, Jan 2006.

[7] S. Berman, Á. Halász, V. Kumar, and S. Pratt, "Bio-inspired group behaviors for the deployment of a swarm of robots to multiple destinations," in *Proc. of the Int. Conf. on Robotics and Automation (ICRA)*, 2007, pp. 2318–2323.

[8] A. Halasz, M. Hsieh, S. Berman, and V. Kumar, "Dynamic redistribution of a swarm of robots among multiple sites," *Intelligent Robots and Systems*, Jan 2007.

[9] M. Feinberg, "Lectures on chemical reaction networks," *Notes of lectures given at the Mathematics Research Center*, 1979.

[10] D. J. Wilkinson, "Stochastic modelling for systems biology," p. 254, Jan 2006.

[11] S. Berman, Á. Halász, M. A. Hsieh, and V. Kumar, "Navigation-based optimization of stochastic deployment strategies for a robot swarm to multiple sites," accepted to 2008 Conf. on Dec. and Control (CDC).

[12] S. Berman, Á. Halász, M. A. Hsieh, and V. Kumar, "Optimal stochastic policies for task allocation in swarms of robots," *IEEE Transactions on Robotics*, 2008, under review.

[13] O. Michel, "Webotstm: Professional mobile robot simulation," *Arxiv preprint cs.RO*, Jan 2004.

[14] D. Gillespie, "A rigorous derivation of the chemical master equation," *Physica A*, Jan 1992.

[15] J. Puchalka and A. Kierzek, "Bridging the gap between stochastic and deterministic regimes in the kinetic simulations of the biochemical reaction networks," *Biophysical Journal*, Jan 2004.

[16] T. Turner, S. Schnell, and K. Burrage, "Stochastic approaches for modelling in vivo reactions," *Computational Biology and Chemistry*, Jan 2004.

[17] N. Correll and A. Martinoli, "Modeling self-organized aggregation in a swarm of miniature robots," *IEEE 2007 International Conference on Robotics and ...*, Jan 2007.

[18] ——, "Robust distributed coverage using a swarm of miniature robots," *Robotics and Automation*, Jan 2007.

[19] ——, "System identification of self-organizing robotic swarms," *Proc. of the Eight Int. Symp. on Distributed Autonomous ...*, Jan 2006.

[20] D. T. Gillespie, "Stochastic simulation of chemical kinetics," *Annual Review of Physical Chemistry*, vol. 58, pp. 35–55, Jan 2007.

[21] H. Li, Y. Cao, and L. Petzold, "Stochkit: A stochastic simulation toolkit," *cs.ucsb.edu*.

[22] M. Chaves, E. D. Sontag, and R. J. Dinerstein, "Steady-states of receptor-ligand dynamics: a theoretical framework," *Journal of theoretical biology*, vol. 227, no. 3, pp. 413–28, Apr 2004.

[23] M. Feinberg, "The existence and uniqueness of steady states for a class of chemical reaction networks," *Archive for Rational Mechanics and Analysis*, Jan 1995.

[24] D. Siegel and D. MacLean, "Global stability of complex balanced mechanisms," *Journal of Mathematical Chemistry*, vol. 27, pp. 89–110, 2000.

[25] R. Heinrich and S. M. Rapoport, "Metabolic regulation and mathematical models," *Prog. Biophys. Molec. Biol.*, vol. 32, pp. 1–82, 1977.

[26] N. Jamshidi and B. O. Palsson, "Formulating genome-scale kinetic models in the post-genome era," *Molecular Systems Biology*, vol. 4, no. 171, pp. 1–10, 2008.

[27] R. Heinrich, S. Schuster, and H.-G. Holzhutter, "Mathematical analysis of enzymic reaction systems using optimization principles," *Eur. J. Biochem.*, vol. 201, pp. 1–21, 1991.

[28] S. Schuster and R. Heinrich, "Time hierarchy in enzymatic reaction chains resulting from optimality principles," *Journal of theoretical biology*, vol. 129, no. 2, pp. 189–209, Nov 1987.

[29] R. Heinrich and S. Schuster, *The Regulation of Cellular Systems*, 1996.

[30] D. P. Landau and K. Binder, *A guide to Monte-Carlo simulations in statistical physics*. Cambridge Univ. Press, 2000.

[31] G. Pólya, "Kombinatorische anzahlbestimmungen für gruppen, graphen und chemische verbindungen," *Acta Mathematica*, Jan 1937.